International Journal of Mechanical Engineering and Technology (IJMET)
Volume 9, Issue 8, August 2018, pp. 438–446, Article ID: IJMET_09_08_048
Available online at http://www.iaeme.com/ijmet/issues.asp?JType=IJMET&VType=9&IType=8
ISSN Print: 0976-6340 and ISSN Online: 0976-6359

DIRECTED ENERGY DEPOSITION OF STEEL 316L: EFFECTS OF BUILD ORIENTATION

Elena Bassoli, Lucia Denti and Andrea Gatto
University of Modena and Reggio Emilia, Dept. of Mechanical and Civil Engineering, Modena, Italy

Neil Thomas Sewell
University of Exeter, School of Engineering, Computing and Mathematics, Exeter, UK

Daniel Johns
Airbus UK, Bristol, UK

ABSTRACT

Metal Additive Manufacturing for the production of end parts is today the major interest in the field of layer-by-layer fabrication. Even if Powder Bed Fusion is by far the most diffused technology, powder-fed systems retain a specific attractiveness, mainly because they enable an easier manufacture of multi-material parts or even of composition-graded ones. These systems, recently categorized by ASTM standards under the term Directed Energy Deposition (DED), still suffer from scarce knowledge of part characteristics and of process robustness and repeatability. Among DED processes, Laser Consolidation (LC) allows the production of net-shape metal parts with good metallurgical soundness, high strength and ductility. As regards the mechanical performance, the non-coaxial architecture of the LC head poses the question of a secondary anisotropy, within each layer, in addition to the primary one that is due to the layerwise construction. The paper addresses the mechanical response and the microstructure obtained by LC with AISI 316L. The direction dependence of part properties is specifically explored. Remarkably high ductility, combined with high hardness and strength, are obtained. The effect of the relative orientation between the LC head and the part is quantified and associated with the observed microstructure.

Keywords: Energy Deposition, Laser Consolidation and Architecture
Cite this Article: Elena Bassoli, Lucia Denti, Andrea Gatto, Neil Thomas Sewell and Daniel Johns, Directed Energy Deposition of steel 316L: effects of build orientation, International Journal of Mechanical Engineering and Technology, 9(8), 2018, pp. 438–446.
http://www.iaeme.com/IJMET/issues.asp?JType=IJMET&VType=9&IType=8

1. INTRODUCTION

Additive Layer Manufacturing (ALM) is an umbrella term used to cover many types of manufacturing where material is used in an additive way to build up 3 dimensional parts. As ALM systems mature, more is expected of the functional parts produced using the technology, especially with respect to accuracy, reliability, repeatability and the mechanical performance. For widespread industrial acceptance, parts need to be produced to high tolerances and with well understood mechanical properties (Bartolo et al., 2008).

Powder-fed processes constitute a new frontier in the field of ALM. Among these, Laser Consolidation (LC) produces net-shape (in this case sheet-like) metal parts without the need for additional finishing. Powder-fed ALM offers promising advantages: metallurgical soundness, high strength and ductility of parts; ease of change of the powder supplied to enable multi-material or graded parts (Domack & Baughman, 2005); operation using standard CNC know-how enabling acceptance in most industries.

Most ALM processes including LC are inherently anisotropic. In particular, the non-coaxial nature of the LC head assembly and the way in which the motion system moves the substrate and existing material are likely to cause direction dependant features varying not only parallel and perpendicular to the build direction, but also within each layer. As a consequence, part performance can be affected by building conditions.

LC uses a laser processing head mounted on the Z-axis of a CNC system. The X- and Y-axes move perpendicular below the Z-axis as the processing head is running to effectively create a continuous deposition of material referred to as the bead. Two additional rotational axes are also available, one around the X axis and one around the Z axis, and can be used for full 5-axis manufacturing if required; however, in these experiments only the three linear axes have been used.

LC is a non-axisymmetric process with powder and laser energy being added in opposing directions focused at a certain distance down from the head unit referred to as the Tool Centre Point (TCP). The TCP occurs at the point the highly divergent laser beam is focused, causing the metal powder to create the molten weld pool. Ideally, the TCP will stay at exactly the correct height from the build surface such that as the build progresses, the head steps away from the X-Y plane at the same rate as the surface builds up. When this is the case, parts build up with smooth regular walls, consistent in width.

Previous work shows that LC parts exhibit excellent mechanical properties (Xue & Islam, 2000) but that the anisotropic nature of the build process leads to anisotropy in the parts produced (Sewell et al., 2008). It is also known that anisotropy exists in similar processes such as Laser Direct Deposition (LDD) and for a variety of metals (Gao et al., 2007, Zhang et al., 2007). Some authors also investigated the effect of anisotropic heat transfer on the final structure and hardness, suggesting that thermal history affects parts and could be modelled and optimized (Costa et al., 2005).

Building upon previous work, this paper looks at the tensile strength and the hardness of parts produced in alternating directions using LC. The results are correlated to parts microstructure and porosity, accounting for the observed anisotropy.

2. MATERIALS AND METHODS

2.1. Part manufacture

The LC system head assembly consists of a non-coaxial powder feeder nozzle and a pulsed Nd:YAG laser. Powder is fed into the building area, melts at the TCP and solidifies as the laser moves on. Building starts on a substrate that is moved beneath the head assembly to produce the first bead. The head unit is raised incrementally to build up the part ideally focusing the beam on the previously built section.

In this experiment, tensile test specimens were constructed, using two different orientations: parallel and orthogonal to the build head. For the specimens with the axis parallel to X direction the head scan during build was parallel to the direction of the laser beam and the powder fed (Figure 1). After manufacturing 7 test samples along the X axis, 5 parts were made along the Y axis, with the head unit moving orthogonally to the head assembly plane. Beads of material were deposited, 180mm long, one on top of another at 0.1mm increments to create rectangular parts just over 20mm high (200 layers). Bead width depends on the amount of powder that consolidates within the laser spot: in this experiment parts were 1mm thick.

Parts were produced using Osprey 316L powder, whose nominal composition is listed in Table 1. In the second part of the table the nominal mechanical properties of sheet 316L of the same producer, obtained by traditional manufacturing processes, are shown to allow for comparison.

LC settings were adopted as determined in preliminary tests for the processing of stainless steel powder (Sewell et al., 2008) and a relative head speed (speed of the head unit along the X or Y axis) of 300mm per minute was used, deliberately lower than usual, to allow for the heat absorbance of the substrate affecting build height for the first 10 layers (Toyserkani & Khajepour, 2006). After this a speed of 375mm per minute was used, also derived from the previous experiments.

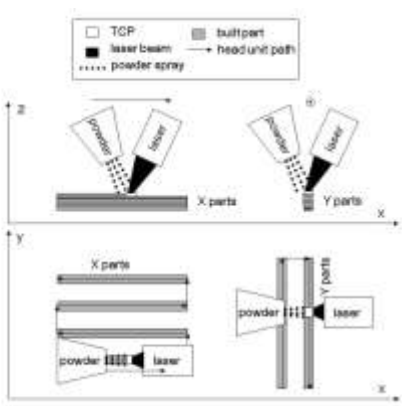

Figure 1 Building strategy in LC.

Table 1 Nominal chemical composition of Osprey 316L powder and mechanical properties of Sandvik 316L sheet.

Chemical composition	**(wt %)**
Cr	16-18
Ni	12-14
Mo	2-3
Mn	1.4
Si	0.7
C	<0.03
Fe	bal.
Mechanical properties	
Young’s Modulus	200 GPa
UTS	485 MPa
Elongation at break	40%
HB	95 (HV10 220 - converted)

The parts were then removed from the substrate along the first few beads as allowed for by the 2mm overbuild added. Waists were added by electro-discharge machining obtaining a geometry consistent with standard BS EN ISO 527-2 (reduced section width 10mm, length 75mm).

2.2. Tests

Ultimate Tensile Strength (UTS) tests were carried out on at least 5 parts in each orientation at a speed of 2mm per minute with strain measured using an extensometer acting on a gage length of 50mm.

Vickers micro-hardness was measured on polished sections of the specimens adopting a load of 200g.

Statistical tools were applied to the evaluation of the mechanical tests results: in particular the t-test for independent samples was used to identify the existence of significant differences between the two groups of specimens.

Then, a deep investigation of rupture and polished sections though optical and scanning electron microscopy allowed the study of the micro mechanisms ruling the macroscopic performances. More in detail, the following observations were carried out:

- Scanning Electron Microscope (SEM) observation of the unprocessed powder, with the aid of EDX semi-quantitative analysis;
- SEM observation of the rupture surfaces to investigate the failure mechanisms;
- Optical microscope (OM) observation of polished sections of unstrained portions of specimens, parallel to the XY plane, before and after chemical etching, to evaluate grain size and distribution;
- Analysis of the OM images before etching to measure parts porosity (50x and 100x – five images for each magnification and building direction).

3. RESULTS AND DISCUSSION

Figure 2 shows an SEM image of the unprocessed powder. The particles are almost spherical. Feret’s and equivalent (Heywood) diameter (Masuda et al., 2006) were measured via image analysis on several SEM pictures, obtaining the cumulative percentage undersize curve shown in Figure 3. The procedure involves the risk of overvaluing the results, due to the effect of particles overlapping, but it is useful to obtain an estimate of the powder granulometry. The measured mean values of Feret’s and equivalent diameter were respectively 40 and 31µm. EDX semi-quantitative analysis was performed on different particles and proved the composition uniformity, with deviations of few percentage points from the values in Table 1.

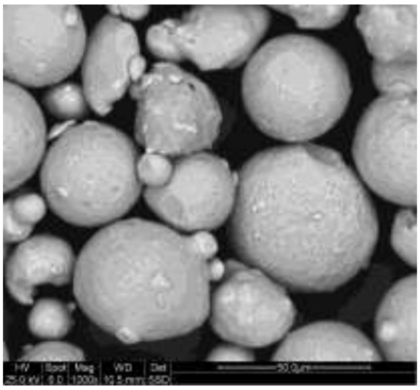

Figure 2 SEM image of the unprocessed Osprey 316L powder.

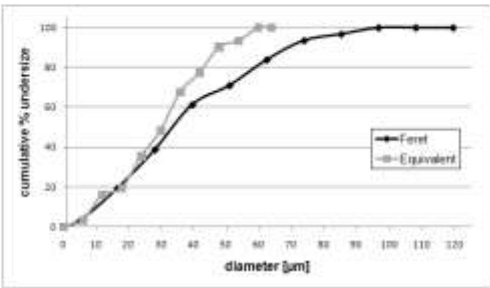

Figure 3 Cumulative percentage undersize curve obtained by image analysis for Osprey 316L powder.

The results of the UTS and micro-hardness tests are listed in Table 2, separately for the X and Y direction. All the specimens exhibited very high strength and hardness, higher than expected for sheet 316L. Elongation at break was inferior than the nominal value for the metal sheet, but excellent for ALM parts. In fact one of the major drawbacks of additive processes is usually parts brittleness, due to inhomogeneities in the built structure. The results also showed a high consistency, especially for the X direction. Figure 4 shows the stress-strain curves of two representative specimens, whose UTS and elongation at break were the nearest to the mean values of the two groups.

The results point out better mechanical performances of the parts produced along the X direction than of Y ones. UTS and hardness are around 6-7% higher for the former, however the difference becomes outstanding as to ductility. Elongation at break for parts built by relative head movement along the plane of LC head assembly is double compared with parts constructed orthogonally.

For a better appreciation of the extent of the described anisotropy, Figure 5 shows the box and whiskers diagrams obtained by the t-test on strength and elongation at break between the two groups of parts. In both cases the presence of a significant anisotropy was proved, being the p values inferior than 0.01.

Table 2 Results of UTS and hardness tests.

	X	**Y**
	mean (SD)	**mean (SD)**
No. Parts	7	5
UTS [MPa]	586 (8.1)	544 (28.4)
εb [%]	32.8 (2.8)	16.6 (6.4)
HV0.2	242 (15,9)	228 (5,7)

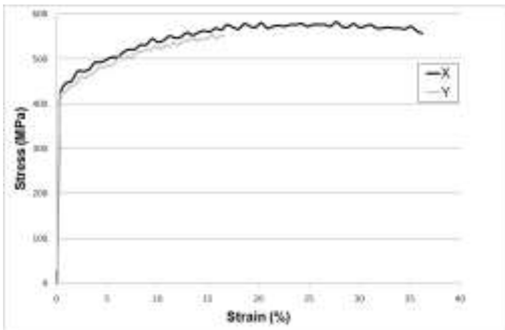

Figure 4 Stress strain curves for a typical X and Y specimen.

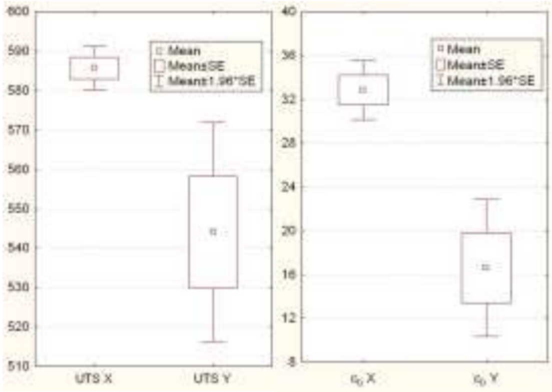

Figure 5 Box & whiskers diagrams resulting from the t-test on UTS and ε_b between X and Y specimens.

Figure 6 illustrates an OM image of a HV0.2 indentation made on an etched section of a Y specimen. Very small grains can be appreciated, with dimensions in the range of few µm. The extremely fine grain structure accounts for the higher mechanical response with respect to the standard sheet material.

Typical rupture surfaces of X and Y direction parts are shown in Figure 7. X specimens (Fig. 7a) exhibit uniform ductile failure morphology based on micro voids forming under strain; porosity previous to rupture is almost absent and joining between the layers is not visible. For Y parts, instead, many large voids are evident throughout the surface (Fig.7b), up to 100μm wide, like the one shown in Figure 8. The smooth inner surface suggests they were formed during laser consolidation.

The amount of voids in the specimens produced in the two configurations was studied in detail through a software for image analysis applied to OM images of XY sections, after binarization. Both X and Y specimens retain a diffused microporosity, with voids smaller than 7μm, visible in Figure 9. Y parts also exhibit much larger pores, as big as the ones observed on the rupture surfaces. The latter were excluded from the porosity measurements, carried out on OM images free from macroscopic defects. The obtained values of percentage microporosity are listed in Table 3. The percentage value is extremely small for X specimens, which are over 99% dense. Microporosity on Y parts is four times bigger, but still around 1%. The two magnifications allow a closer or wider look of the microstructure, so the higher porosity measured at 100x (the same as in Fig. 9) denotes the presence of microvoids that are not visible at lower enlargements.

Two distinct disparities were thus observed as to porosity on parts produced in the two directions. The first is a diffused microporosity, which appears to be intrinsic in the technology and in Y parts is almost 4 times higher than in X specimens. Secondly, parts produced in the Y direction show macropores that are absent in X parts. The latter can be regarded as defects. The two effects together account for the observed discrepancy in the mechanical characteristics. In Y direction the powder is sprayed across and not along the section being built, which can likely be the cause for less material consolidated in the building area. Building in X direction the speed vector causes the powder particles to remain in the build area for a longer time, so that the probability for a particle to be caught by the laser spot and melted is higher than if the speed is perpendicular to the consolidated bead and to the path of the weld pool.

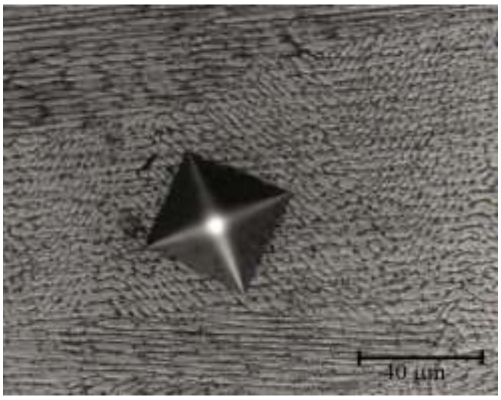

Figure 6 OM image of a micro-indentation.

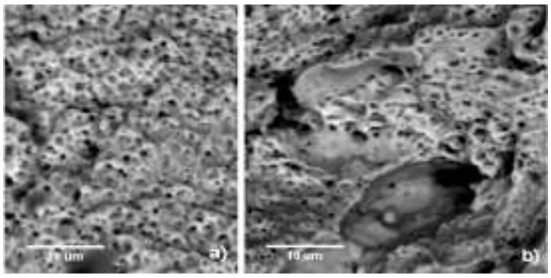

Figure 7 Rupture surface: a) X part; b) Y part.

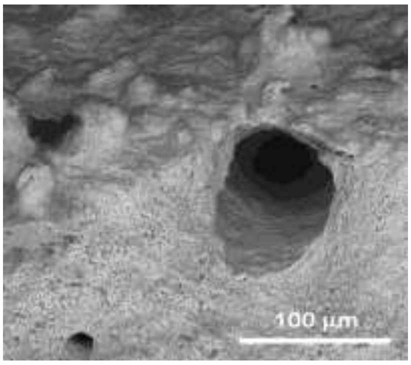

Figure 8 Rupture surface of a Y specimen.

Table 3 Percentage porosity measured on X and Y specimens.

	X	**Y**
Porosity [%]	mean (SD)	mean (SD)
50x	0.22 (0.1)	0.84 (0.7)
100x	0.36 (0.2)	1.32 (1.2)

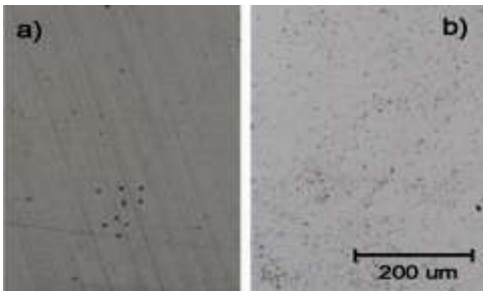

Figure 9 OM images for porosity measurement (100x): a) X specimen; b) Y specimen.

4. CONCLUSIONS

In conclusion, this study confirmed that LC parts show high mechanical properties, equal to or better than parts produced traditionally. In particular, ductility is remarkably high compared with other additive processes. Anisotropy within the building plane was analysed, finding that the specimens created in the X direction exhibit higher strength and hardness as well as much higher ductility when compared with parts created in the Y direction. The distinction between the two was proved through statistical tests. Moreover, the parts in the X direction demonstrated consistent results throughout the test samples, whereas the parts in the Y direction displayed greater variation between the results.

SEM observation of the rupture surfaces revealed ductile failure morphology. Numerous voids were observed on the rupture surfaces of the parts in the Y direction, in the range of 100 µm.

The percentage residual porosity was quantified through image analysis of polished sections. A diffused microporosity is present in both kind of specimens, constituted of pores of few µm. X specimens are over 99% dense. Microporosity on Y parts, even if four times greater than on X parts, is still around 1%. Yet, macropores can be observed as well on Y specimens. The two results together justify the difference in the tensile properties, in particular as to the lower ductility of Y parts.

The major finding of the research is that the relative orientation between the powder speed vector and the building path was proved to influence the mechanical response, due to a different probability of the powder to be involved by the laser spot, which results in a different amount of consolidated material per section. OM and SEM observation allowed investigating the microstructural anisotropies. Two combined mechanisms were identified, at the micro- and macro-scale, accounting for the observed anisotropy between parts built in the two studied orientations.

As a direct consequence of this research, a specific CNC programming technique employing the rotational axis of the worktable could ensure the feed vector to be parallel to the LC head assembly, obtaining an optimization of parts mechanical response. This work is currently being undertaken.

Future developments of the research will regard a deeper investigation of heat and material flows, of the building phenomena and of their effects on parts microstructure in the three directions in space.

ACKNOWLEDGEMENTS

Parts for testing were manufactured using the Accufusion Laser Consolidation System, owned by Airbus and based at the University of Exeter. This system is currently involved in a UK Government Technology Strategy Board sponsored project, named DAMASCUS, to investigate the ALM of parts for aerospace and automotive. Samples were tested, prepared and examined at the University of Modena and Reggio Emilia.

REFERENCES

[1] Bartolo et al. (eds) 2008. Virtual and Rapid Manufacturing. London: Taylor and Francis Group.

[2] Costa, L.; Vilar, R.; Reti, T. & Deus, A.M. 2005. Rapid tooling by laser powder deposition: Process simulation using finite element analysis, Acta Materialia 53 (14): 3987-3999.

[3] Domack, M.S. & Baughman, J.M. 2005. Development of nickel-titanium graded composition components. Rapid Prototyping J. 11 (1): 41 - 51.

[4] Gao, S.Y.; Zhang, Y.Z.; Shi, L.K.; Du, B.L.; Xi, M.Z. & Ji, H.Z. 2007. Research on Laser Direct Deposition Process of Ti-6Al-4V Alloy. Acta Metall. Sinica (English Letters) 20 (3): 171-180.

[5] Masuda, H.; Higashitani, K. & Yoshida, H. (3rd ed.) 2006. Powder technology handbook. CRC/Taylor & Francis

[6] Sewell, N.T.; Bassoli, E.; Gatto, A. & Evans, K.E. Additive Layer Manufacture of Tensile Tests Specimens in Stainless Steel 316L by Laser Consolidation. iCAT 2008, September 17th – 18th 2008, Ptuj, Slovenia.

[7] Toyserkani, E & Khajepour, A. 2006. A mechatronics approach to laser powder deposition process. Mechatronics 16 (10): 631-641.

[8] Xue, L. & Islam, M.U. 2000. Free-form laser consolidation for producing metallurgically sound and functional components. J. of Laser Applications 12 (4): 160-165.

[9] Zhang, K.; Liu, W. & Shang, X. 2007. Research on the processing experiments of laser metal deposition shaping. Optics & Laser Technology 39: 549–557.